VILNIUS UNIVERSITY

CENTER FOR PHYSICAL SCIENCES AND TECHNOLOGY

INSTITUTE OF CHEMISTRY

Ieva Matulaitienė

VIBRATIONAL SPECTROSCOPIC STUDY ON THE STRUCTURE AND INTERACTION WITH SOLUTION COMPONENTS OF MONOLAYERS WITH PYRIDINIUM FUNCTIONAL GROUP ADSORBED ON METAL SURFACE

Summary of Doctoral dissertation

Physical sciences, Chemistry (03 P)

Vilnius, 2013

The research was prepared at the Center for Physical Sciences and Technology / Institute of Chemistry in the period of 2008–2012.

Scientific supervisor:

habil. dr. **Gediminas Niaura** (Center for Physical Sciences and Technology, physical sciences, chemistry – 03 P)

Doctoral dissertation is defended at the Evaluation board of Chemistry of Vilnius University:

Chairman:
Prof. habil. dr. **Albertas Malinauskas** (Center for Physical Sciences and Technology, physical sciences, chemistry – 03 P)

Members:
Dr. **Justas Barauskas** (Malmö University (Sweden), physical sciences, biochemistry – 04 P;
Prof. habil. dr. **Eugenijus Butkus** (Vilnius University, physical sciences, chemistry – 03 P);
Prof. dr. **Šarūnas Meškinis** (Kaunas University of Technology, technological sciences, materials engineering – 08 T);
Prof. habil. dr. **Eugenijus Norkus** (Center for Physical Sciences and Technology, physical sciences, chemistry – 03 P)

Opponents:
Dr. **Audrius Misiūnas** (Center of Pharmaceutical Biotechnology „Biotechpharma", physical sciences, chemistry – 03 P);
Prof. habil. dr. **Rimantas Vaišnoras** (Lithuanian University of Educational Science, physical sciences, physics – 02P)

The dissertation defense will take place at 11 a.m. on December 27th, 2013 at the public meeting of the Evaluation board at the Assembly Hall the Center for Physical Sciences and Technology / Institute of Chemistry.
    Address: A. Goštauto 9, LT – 01108, Vilnius, Lithuania.

The summary of the dissertation has been sent on November 27th, 2013.

The doctoral thesis is available at the library of Center for Physical Sciences and Technology and at the library of Vilnius University.

VILNIAUS UNIVERSITETAS

FIZINIŲ IR TECHNOLOGIJOS MOKSLŲ CENTRAS

CHEMIJOS INSTITUTAS

Ieva Matulaitienė

ADSORBUOTŲ ANT METALO PAVIRŠIAUS MONOSLUOKSNIŲ SU PIRIDINIO FUNKCINE GRUPE STRUKTŪROS IR SĄVEIKOS SU TIRPALO KOMPONENTAIS TYRIMAS VIRPESINĖS SPEKTROSKOPIJOS METODAIS

Daktaro disertacijos santrauka

Fiziniai mokslai, chemija (03 P)

Vilnius, 2013

Disertacija rengta 2008 – 2012 metais Fizinių ir technologijos mokslų centro Chemijos institute

Mokslinis vadovas:

habil. dr. **Gediminas Niaura** (Fizinių ir technologijos mokslų centras, fiziniai mokslai, chemija – 03 P).

Disertacija ginama Vilniaus universiteto Chemijos mokslo krypties taryboje:

Pirmininkas:
    Prof. habil. dr. **Albertas Malinauskas** (Fizinių ir technologijos mokslų centras, fiziniai mokslai, chemija – 03P).

Nariai:
    Dr. **Justas Barauskas** (Malmės universitetas (Švedija), fiziniai mokslai, biochemija – 04P);
    Prof. habil. dr. **Eugenijus Butkus** (Vilniaus universitetas, fiziniai mokslai, chemija – 03P);
    Prof. dr**. Šarūnas Meškinis** (Kauno technologijos universitetas, technologijos mokslai, medžiagų inžinierija – 08T);
    Prof. habil. dr. **Eugenijus Norkus** (Fizinių ir technologijos mokslų centras, fiziniai mokslai, chemija – 03P)

Oponentai:
    Dr. **Audrius Misiūnas** (UAB Biotechnologinės farmacijos centras „Biotechpharma", fiziniai mokslai, chemija – 03P);
    Prof. habil. dr. **Rimantas Vaišnoras** (Lietuvos edukologijos universitetas, fiziniai mokslai, fizika – 02P)

Disertacija bus ginama viešame Chemijos mokslo krypties tarybos posėdyje 2013 m. gruodžio mėn. 27 d. 11 val. Fizinių ir technologijos mokslų centro Chemijos instituto aktų salėje.
        Adresas: Goštauto 9, LT – 2600, Vilnius, Lietuva

Disertacijos santrauka išsiuntinėta 2013 m. lapkričio mėn. 27 d.

Disertaciją galima peržiūrėti Fizinių ir technologijos mokslų centro Chemijos instituto ir Vilniaus universiteto bibliotekose

INTRODUCTION

Self-assembled monolayers (SAMs) provide possibility of changing metal surface properties in controllable manner and are widely used in studies of electron transfer, construction of (bio)sensors, and biotechnological and photoelectronic processes. Positively charged monolayers are valuable in development of sensors for anions and (bio)technological processes with adsorbed negatively charged macromolecules [1, 2]. Contrary to covalent wired peptides and proteins, electrostatically attracted biomolecules more readily preserve their native structure and function at interface because of unrestricted mobility.

The use of amines in the construction of positively charged surfaces is common [1, 3]. However, these compounds have multiple disadvantages. First of all, it is possible to work only at special conditions, in acid or weak acid solutions [4]. Secondly, the amine group is able to interact with the substrate metals (Au, Ag) or with specifically adsorbed anions on the electrode surface [5]. SAMs with terminal pyridinium functional group offer positive charge at interface in a wide solution pH range. Thus, Abell and co-workers have synthesized the merkaptoheksil pyridinium bromide and used it for the construction of three-dimensional (3D) structures [6]. The electrostatic attraction of proteins, construction of poly-layered structures, and immobilization of quantum dots was demonstrated [6–9].

The functional performance of monolayers depends on the structure and stability of surface attached organic molecules. Thus, for construction of surfaces with particular and predictable properties, detailed molecular level knowledge on the structure and function of the monolayers are required. In this work surface enhanced Raman spectroscopy (SERS) was used for molecular level analysis of structure and function of self-assembled monolayers with positively charged pyridinium functional group. SERS is one of the most sensitive vibrational spectroscopic tools for probing the bonding, structure, and orientation of adsorbed molecules at certain nanostructured metals (mostrly Au, Ag, and Cu) with molecular specificity and submonolayer sensitivity.

The aims of this work is to get better insight into the molecular structure and interactions of monolayer formed from of N-(6-Mercapto)hexylpyridinium (MHP) molecules with inorganic ions, dodecylsulfate anion, and graphene oxide.

The main objectives of the work were as follows:

1. To establish stable monolayers of MHP molecules on Au and Ag electrodes;

2. To make assignments of MHP monolayer SERS bands based on isotopic substitution and quantum chemistry calculations;

3. To evaluate SERS marker bands of MHP structure and orientation with respect to the electrode surface;

4. To determine the effect of electrochemical potential on the molecular structure of MHP monolayer;

5. To investigate peculiarities of formation of ion pairs between the MHP monolayer and inorganic ions in solution;

6. To establish the detection limit of ClO_4^- ions in solution by using SERS method and MHP monolayer;

7. To determine peculiarities of interaction of graphene oxide with MHP monolayer;

8. To determine the effect of electrochemical potential on the structure of adsorbed graphene oxide.

The novelty and significance of the work

The positive-charge-bearing self-assembled monolayer of N-(6-mercapto)hexylpyridinium (MHP) molecules was formed on Au and Ag electrodes. The molecular structure of monolayer was probed by surface-enhanced Raman spectroscopy (SERS). Based on quantum chemical calculations, isotopic substitution, immersion time- and temperature-dependent experiments, the specific SERS marker bands for structure and orientation of MHP molecules were evaluated. A band near 1083 cm^{-1} has been assigned to C–C stretching vibration of hydrocarbon chain in all-trans conformation. Based on dependence of relative intensity-electrode potential profiles on excitation wavelength the operation of charge transfer resonant Raman enhancement mechanism in Au/MHP system was suggested. It was demonstrated that MHP monolayer effectively attracts inorganic anions as well as dodecyl sulfate ion from aqueous solution. The detection limit for perchlorate anion was found to be 10^{-8} M. The downshift in frequency of totally symmetric stretching mode of anions due to the formation of ion pairs at

interface was detected by SERS. The higher shift was found to be correlated with the large Gibbs dehydration energy of anion. The reduced graphene oxide was prepared at interface of Au modified by MHP and SERS was employed to probe in situ the potential induced changes in parameters of D and G bands. It was found that both D- and G-band wavenumbers linearly depends on the potential. The effect was explained in terms of changes in the C$-$C bond length induced by the electrochemical doping. The positive-charge-bearing MHP monolayer on Au and Ag surfaces might be utilized in various electrochemical applications.

The defense statements of the work:

1. SERS band of adsorbed MHP at 1083 cm^{-1} belongs to C$-$C stretching vibration of hydrocarbon chain in all-trans conformation;

2. An additional charge transfer resonance Raman enhancement mechanism operates in the Au/MHP system;

3. The shift in frequency of the totally symmetric stretching vibration of adsorbed anions comparing with the corresponding mode of ions in solution correlates with the Gibbs dehydration energy;

4. The MHP monolayer provides possibility to detect the ClO_4^- ions in solution by SERS method at 10^{-8} M concentration level;

5. Dodecylsulfate ions adsorb at MHP monolayer in the configuration providing the interaction of sulfate group with the pyridinium ring.

6. The MHP monolayer attracts negatively charged graphene oxide;

7. The electronic structure and length of C$-$C bonds of adsorbed reduced graphene oxide can be altered by electrochemical potential.

List of publications:

1. **I. Matulaitienė**, J. Barkauskas, R. Trusovas, G. Račiukaitis, R. Mažeikienė, O. Eicher-Lorka, G. Niaura. Potential dependence of SERS spectra of reduced graphene oxide on self-assembled monolayer at gold electrode. Chemical Physics Letters, http://dx.doi.org/10.1016/j.cplett.2013.10.068.

2. **I. Matulaitienė**, L. Abariūtė, Z. Kuodis, O. Eicher-Lorka, A. Matijoška, G. Niaura. Electrostatic binding of ions by self-assembled monolayer of N-(6-mercapto)hexylpyridinium on Ag electrode as probed by surface enhanced Raman spectroscopy. Chemija, (in press).

3. V. Voiciuk, G. Valincius, R. Budvytytė, A. Matijoška, **I. Matulaitienė**, G. Niaura. Surface-enhanced Raman spectroscopy for detection of toxic amyloid β oligomers adsorbed on self-assembled monolayers. Spectrochimica Acta Part A: Molecular and Biomolecular Spectroscopy, 95 (2012) 526–532.

Submitted manuscript:

1. **I. Matulaitienė**, Z. Kuodis, A. Matijoška, O. Eicher-Lorka, G. Niaura. SERS characterization of the positive charge bearing N-(6-mercapto)hexylpyridinium self-assembled monolayer on gold electrode. Journal of Electroanalytical Chemistry (submitted).

Contribution report to the publications

1. I did all experimental work, except the synthesis of grapheme oxide, also participated in data evaluation and interpretation.

2. I did most experimental work and participated in data evaluation and interpretation.

3. I did experimental work for attraction of inorganic anions by MHP and participated in providing assignments of MHP vibrational modes.

Submitted manuscript. I did most experimental work and participated in data evaluation and interpretation.

Conference materials

1. **I. Matulaitienė**, O. Eicher-Lorka, Z. Kuodis, L. Abariūtė, G. Niaura. SERS study of the interaction of anions with positive charge bearing mercaptohexylpiridinium monolayer on gold and silver electrodes. *Chemistry*. 2013, September. Vilnius.

2. **I. Kairytė**, Z. Kuodis, A. Matijoška, O. Eicher-Lorka, L. Abariūtė, G. Niaura. Surface-enhanced Raman spectroscopic study of adsorption of mercaptohexylpyridinium on gold electrode. *Organic Chemistry*. 2010, April. Kaunas.

3. **I. Kairytė,** Z. Kuodis, A. Matijoška, O. Eicher-Lorka, G. Niaura. SERS study of the interaction of perchlorate anion with positive charge mercaptohexylpiridinium monolayer on gold electrode. *Chemistry*. 2011, October. Vilnius.

4. **I. Kairytė**, Z. Kuodis, A. Matijoška, O. Eicher-Lorka, G. Niaura. Characterization of positive charge bearing mercaptohexylpyridinium SAM at gold electrode. *ERPOS-12*. 2011, July. Vilnius.

5. **I. Kairytė**, Z. Kuodis, A. Matijoška, O. Eicher-Lorka, L. Abariūtė, G. Niaura. Surface-enhanced Raman spectroscopic study of electrostatic attraction of anions by mercaptohexylpiridinium monolayer. *Organic Chemistry*. 2011, April. Kaunas.

MATERIALS AND METHODS

Materials

Millipore-purified water (18 MΩ cm) was used for preparation of solutions. Deuterium oxide (99.9 atom % D) was obtained from Sigma Aldrich. The most inorganic salts were ACS reagent grade and were purchased from Sigma-Aldrich Chemie GmbH (Germany). Sulfamic acid and sodium tetrafluoroborate were of "chemically pure" category, and they were acquired from RIAP (Kiev, Ukraine) and Reachim (Moscow, Russia), respectively. The sodium hexafluorophosphate was from Strem Chemicals, Inc. (Newburyport, MA). Graphite used for the synthesis was of extra pure grade (Merk), other chemicals were of analytical grade. GO was synthesized using the Hummer's method [10]. N-(6-mercapto)hexylpyridinium (MHP) chloride (Figure 1) was modified and synthesized in our laboratory by dr. Olegas Eicher-Lorka and dr. Algis Matijoška, respectively (Department of Organic Chemistry, Center for Physical Sciences and Technology). The same synthesis scheme (Fig. 1) was used for synthesis of MHP analog, with deuterated pyridinium ring.
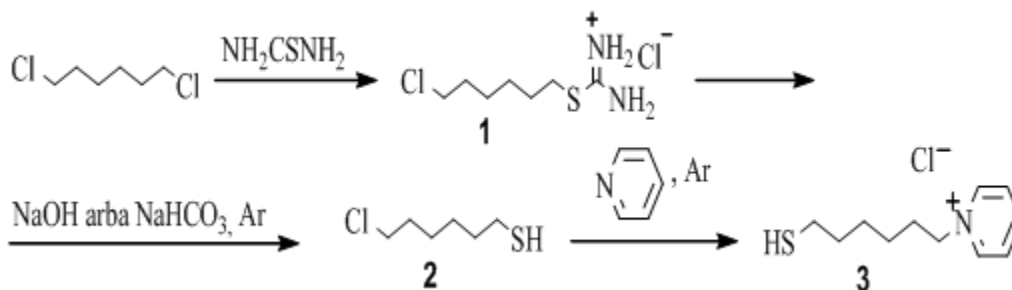
Fig. 1. Synthesis rote of N-(6-mercapto)hexylpyridinium (MHP) chloride (compound **3**).

Raman spectroscopy measurements

Raman and surface-enhanced Raman scattering (SERS) measurements were conducted with an Echelle type spectrometer RamanFlex 400 (PerkinElmer, Inc.) equipped with a thermoelectrically cooled (-50 ^{o}C) CCD camera and fiber optic cable for excitation and collection of the Raman spectra. The near-infrared diode laser provided excitation beam at 785 nm. The excitation-scattering geometry was 180°. The laser power at the sample was restricted to 30 mW and the beam was focused to a 200 µm diameter spot on the metal surface. The integration time was 300 s. Measurements in solution were performed in a cylindrical glass cell with a quartz window. In order to reduce photo- and thermo-effects on the sample, the cell holder together with the working electrode was moved periodically with respect to the laser beam at a rate of about 15−25 mm/s with the help of custom build equipment [11]. The wavenumber axis was calibrated by the polystyrene standard ASTM E1840, yielding $\pm$ 1 cm^{-1} accuracy for narrow bands. Raman intensities were corrected by the NIST intensity standard SRM 2241. Parameters of overlapped bands were determined by fitting the experimental contour with Lorentzian-Gaussian form components by using the Grams/AI 8.0 software (Thermo Scientific Corp.).

Electrode preparations

Au an Ag electrodes were used for SERS measurements. The metal rod was pressed into Teflon and pretreated in the following ways. The Ag electrode was polished with soft sandpaper (P2500) and 0.3 µm alumina slurry (Buehler, USA) for refreshing the surface and sonicated in water-methanol mixture (1:1, v/v) for 10 min. Then the electrode was roughened in 0.1 M KCl solution using four oxidation−reduction cycles in the potential range between −0.40 and 0.40 V vs. Ag/AgCl/KCl−saturated (scan rate

1200 mV/s) with pause for 30 s at the negative and 30 s at the positive potentials. The Au electrode also was polished with soft sandpaper (P2500) and 0.3 μm alumina slurry (Buehler, USA) for refreshing the surface and sonicated in water-methanol mixture (1:1, v/v) for 10 min. Then it was cleaned electrochemically by potential cycling in 0.5 M H_2SO_4 between 0.4 and 1.6 V at 100 mV/s scan rate for 30 cycles. After cleaning procedures it was roughened in 0.1 M KCl solution by 50-fold scanning the potential from −0.30 to 1.30 V (sweep rate 500 mV/s with holds of 90 s at the negative potential and 2 s at the positive one). SAMs were formed by incubation of SERS active substrate in acetonitrile solution containing 10^{-3} M MHP for a certain period of time. After that the electrode was rinsed in acetonitrile, dried and transferred to the spectrometer stage holder for SERS measurements. SERS measurements were conducted *in situ* in aqueous solutions.

Theoretical modeling

Theoretical modeling and calculations were performed using Gaussian for Windows package version G03W [12]. Geometry optimization and frequency calculations were accomplished with the density functional theory (DFT) method using the B3LYP functional and 6-31++G(d,p) basis set for C, H, N, and S atoms, and LANL2DZ with ECP for Au and Ag atoms. Calculated frequencies were scaled by the relation: $\nu'=\alpha(\nu)\cdot\nu$, where ν' and $\alpha(\nu)$ is the scaled frequency and scaling factor, respectively. The scaling factor was defined by the following equation [13]:

$$\alpha(\nu) = 1 - (1 - \alpha^F) \frac{\nu - \nu^0}{\nu^F - \nu^0} \qquad (1)$$

using the parameters: $\alpha^F=0.97$, $\nu^F=4000$, and $\nu^0=600$.

Calculated Raman scattering activities (S_j) were scaled by converting them to the Raman cross sections (Mσ/Ω) which are proportional to the Raman intensities and can be compared with the experimental data. The Raman scattering cross sections were calculated by using the following equation [14, 15]:

$$\frac{\partial \sigma_j}{\partial \Omega} = \left(\frac{2^4 \pi^4}{45}\right) \left(\frac{(\nu_0 - \nu_j)^4}{1 - \exp\left[\frac{-hc\nu_j}{kT}\right]}\right) \left(\frac{h}{8\pi^2 c\nu_j}\right) S_j, \qquad (2)$$

where ν_0 is the laser excitation frequency, ν_j is the vibrational frequency of the *j*th normal mode, and *c* and *k* are the universal constants. Predicted vibrational spectra were

11

generated by using Lorentzian function for broadening of Raman lines with 4 cm^{-1} full width at half-maximum (FWHM) values.

Calculations were performed in collaboration with dr. O. Eicher-Lorka (Center for Physical Sciences and Technology).

RESULTS AND DISCUSSION

Asignments of MHP bands

The Mercaptohexylpyridinium (MHP) molecule consists of three molecular units: thiol group, polymethylene chain ($-CH_2)_6-$), and charged pyridinium group (Fig. 2). Each group can be characterized by Raman spectroscopy. SERS measurements were performed at Au and Ag electrodes. To clarify assignments of the SERS bands we have conducted the first principles quantum chemical calculations of structure and vibrational spectrum of complexes Au$_3$-MHP, Ag$_3$-MHP (Fig. 2 A, B).
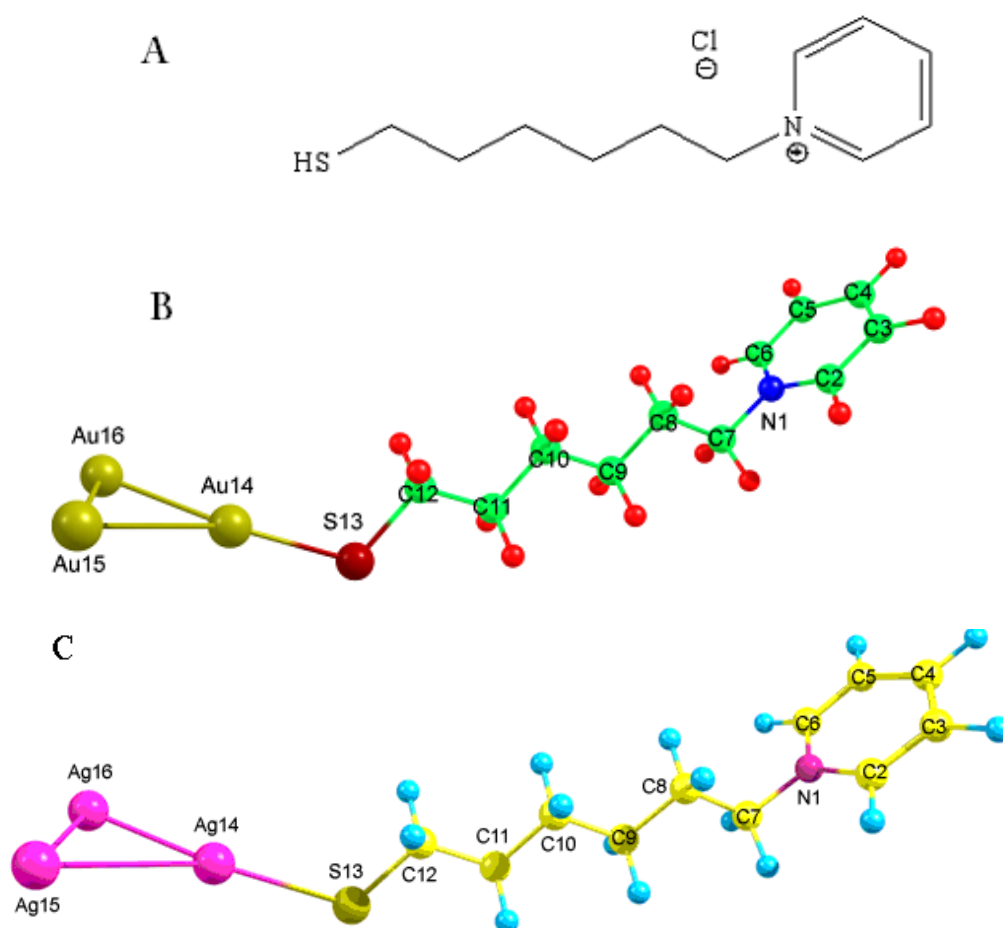
Fig. 2. Structure of N-(6-mercapto)hexylpyridinium (MHP) (A), structures of MHP complex with three gold (B) and silver (C) atoms optimized at DFT/B3LYP/6-31++G(d, p) level for C, H, N, and S atoms and LANL2DZ with ECP for Au and Ag atoms.

Figure 3 compares Raman spectra of aqueous MHP (0.5 M) solution with SERS spectrum of this compound adsorbed at Au electrode, and calculated spectrum in the spectrum regions of 200–1700 cm^{-1} and 2500–3200 cm^{-1}. Assigments of the bands based on previous studies of similar compounds [16–25] of our own calculations are displayed in Table 1. In SERS and Raman spectra dominates trigonal ring breathing mode at 1028 cm^{-1} (ν_{12}). Several Pyridinium ring vibrational modes experience clear shift to lower wavenumbers upon adsorption of MHP on Au (Fig. 3, A). It concerns the high frequency ν(=C–H) vibrational mode near 3077 cm^{-1}, and for well-defined ν_{8a}, ν_{8b}, ν_{9a}, and ν_{15} modes located in SERS spectrum at 1627, 1579, 1210, and 1174 cm^{-1} respectively. The characteristic pyridinium ring in-plane bending vibration (ν_{6b}) appears at 648 and 646 cm^{-1} in solution and surface spectrum, respectively. Also the similar MHP vibrational modes and their shifts were observed on Ag.

The most intensive bands of hydrocarbon chain of MHP ($-(CH_2)_6-$) are located in the high frequency spectral region (2800–3000 cm^{-1}), they are associated with C–H stretching vibrations of methylene groups (Fig. 3, B). However, Fermi resonance with methylene groups bending vibrational phenomena complicates assignment of these bands [18]. Presence of bands near 2857 and 2915 cm^{-1} in SERS spectra is characteristic for bifunctional alkanethiols adsorbed at Au substrate [20, 26]. Calculations have revealed that the high frequency shoulder observed at 2978 and 2959 cm^{-1} in solution and SERS spectra, respectively, corresponds to symmetric stretching vibration of methylene group adjusted to pyridinium ring (Table 1). In solution spectrum, the scissoring bending vibration of methylene groups is visible at 1443 cm^{-1} (Figure 3).

Comparison of Raman and SERS bands of pyridinium ring and hydrocarbon chain reveals that adsorption of MHP on metal surface induces theese changes: 1) frequencies of pyridinium ring modes decrease; 2) bandwidth increase; 3) relative intensities of hydrocarbon chain modes decrease comparing to pyridinium ring modes.
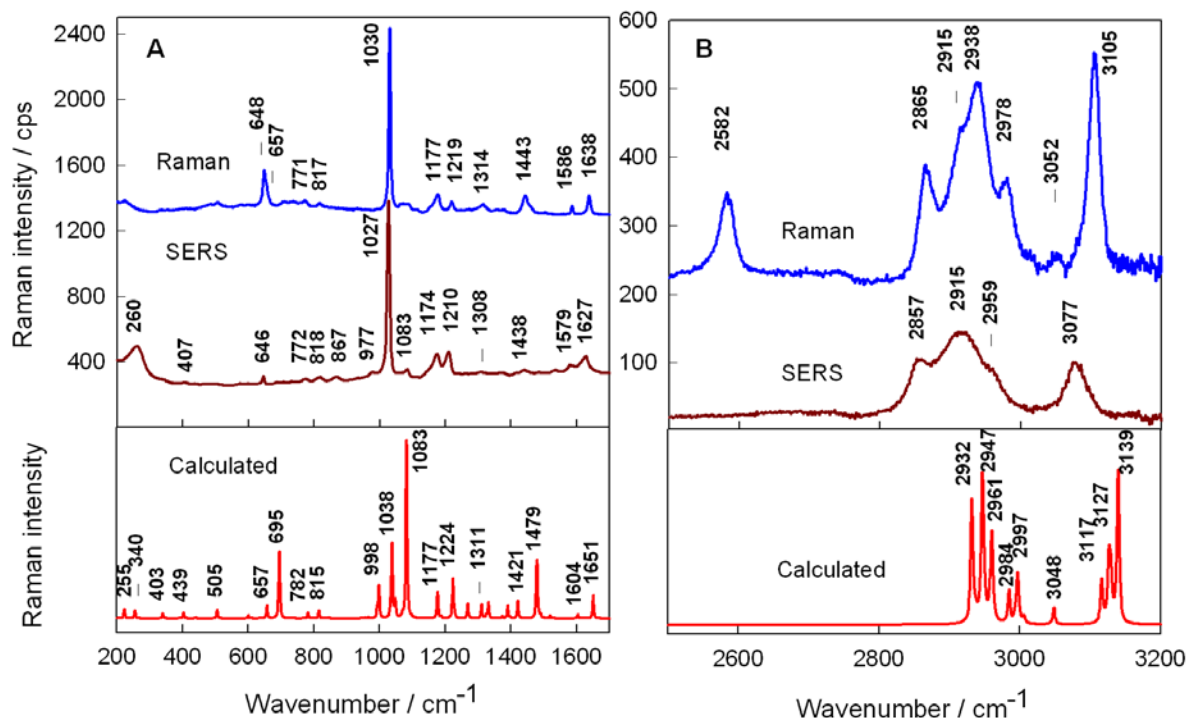
Fig. 3. Comparison of aqueous solution (0.5 M) Raman spectrum of MHP, SERS spectrum of MHP adsorbed at Au electrode, and calculated spectrum of Au$_3$-MHP complex performed at DFT/B3LYP/6-31++G(d, p) level for C, H, N, and S atoms and LANL2DZ with ECP for Au atoms in the spectrum regions of 200–1700 cm^{-1} (A) and 2500–3200 cm^{-1} (B). Experimental spectra were normalized according to pyridinium ring ν_1 mode near 1030 cm^{-1}. Water spectrum was subtracted from solution spectrum of MHP. Excitation wavelength is 785 nm.

Table 1. Wavenumbers, depolarization ratios, and assignments of vibrational bands of MHP in solution and adsorbed state

Raman		SERS		Calculated	Assignments
0.5 M MHP solution		Au/MHP (in air)	Au/MHP-D$_5$ (in 0.1 M NaClO$_4$ solution)	(Au$_3$-MHP)	
ν	ρ				
3105 s	0.14	3077 s	2315 m	3139	ν(=C–H) ring in-phase [ν_2 (A$_1$)]^c
2978 m	0.10	2959 m	2964 sh	2997	ν_s(C7H$_2$) methylene group near ring
2938 s	0.08	n.o.	n.o.	n.a.	ν_s(CH$_2$)$_{FR}$ chain
2916 sh	0.17	2915 s	2911 s	2959	ν_{as}(CH$_2$) chain
2865 m	0.04	2857 m	2866 m	2931	ν_s(CH$_2$) chain
2582 m	0.10	n.a.	n.a.	n.a.	ν(S–H)
1638 m	0.63	1627 m	1592 w	1651	ν(C2=C3) + ν(C6=C5) [8a(A$_1$)]
1586 w	0.63	1579 w	1551 w	1604	ν_{as}(C3C4C5) + ν_{as}(C2N1C6) [8b(B$_2$)]
1443 m	0.69	1438 m	1440	1480	δ(CH$_2$) scissoring, chain
1314 w	n.d.	1308 w	1306 w	1311	twist(CH$_2$) chain
1219 w	0.41	1210 s	868 m	1229	β(CH) ring [9a(A$_1$)]

14

1177 m	0.15	1174 m	1132 m	1177	ν(C7–N1) + β(CH) ring
1086 w, sh	0.18	1083 w	1083 m	1083	ν_s(C–C)$_T$ in-phase all-trans chain
1064 w, sh	0.31	1063 w, sh	1070 w, sh	n.a.	ν(C–C)$_G$
1030 vs	0.04	1027 vs	989 vs	1038	ν_s(CCN) trigonal ring breathing [12(A$_1$)]
n.d.	n.d.	867 m	n.d.	993	ν(C–C) / rock(CH$_2$) chain
817 w	p	818 w	764 w	815	ν(C7–N1) + δ(C3C4C) ring in-plane
771 w	n.d.	772 w	n.d.	782	γ(CH) ring [10b(B$_1$)]
732 w	n.d.	703 w	703	695	ν(C–S)$_T$ + rock(CH$_2$) chain
710 w	n.d.	n.d.	n.d.	737/692	rock(CH$_2$) chain / γ(CH) ring
657 sh, m	n.d.	n.d.	n.d.	n.a.	ν(C–S)$_G$
648 m	0.42	646 m	620	658	δ(CCC) ring in-plane [6b(B$_2$)]
505 w	n.d.	n.d.	459 w	506	γ(CCN) ring
n.a.	n.a.	407 w	402	403	δ(Au–S–C)
n.a	n.a	260 m	265 m	255	ν(Au–S)

[a]Based on references [16–25] and calculations; [b]calculated at B3LYP/6-311++g(2d,p) level with hydrocarbon chain in trans conformation; [c]Wilson vibration number of the benzene ring and vibration symmetry. Abbreviations: ν – stretching; ν_s – symmetric stretching; ν_{as} –asymmetric stretching; δ – deformation; β – in-plane bending; γ – out-of-plane bending; s – strong; vs – very strong; m – middle; w – weak; sh – shoulder; n.d. – not determined; n.a. – not applicable; T − *trans*; G − *gauche*; FR – Fermi resonance.

MHP bonding on Au and Ag surfaces is different

Upon MHP adsorption to metal surface S−H bond dissociates, and well-defined feature at 2582 cm^{-1} in solution spectrum due to S−H stretching mode of thiol group disappears in the surface spectrum. Direct evidence on chemisorption of MHP at surface provides low frequency metal−sulfur and C−S stretching vibration spectral regions (Fig. 4). It is known that metal nature affects the strength of the metal-sulfur and C−S bonds as well as alignment of C−S bond [18]. Well-defined bands at 236 and 260 cm^{-1} belong to Ag−S and Au−S stretching modes, respectively. First principle quantum chemical calculations performed by modeling the silver and gold surface with cluster of three atoms predict metal−sulfur vibrational modes at 230 and 255 cm^{-1}, respectively (Table 2). Higher frequency of ν(Au−S) vibration correlates with shorter Au−S calculated bond length (2.35 Å) comparing with silver (2.58 Å) electrode.

The thiol group has other characteristic, which resembles the C–S stretching mode, and that is also sensitive to *gauche/trans* isomerization of −CH$_2$−CH$_2$−S− moiety [18,

19]. The well-defined band is visible near 692 cm^{-1} in the case of Ag electrode upon adsorption due to $\nu(C-S)_T$ vibration, while in the spectrum from Au substrate the low intensity feature appears at 696 cm^{-1} (Fig. 4). In the spectrum from Ag/MHP monolayer the band from gauche conformer, $\nu(C-S)_G$, is clearly visible at 630 cm^{-1}. Analysis of relative intensities ($I_{\nu(C-S)T}/I_{\nu(C-S)G}=2.3$) indicated dominance of *trans* conformer at interface of Ag electrode. Upon adsorption of MHP due to interaction with electrode induced withdrawal of electron density from the C−S bond and metal mass effect [18, 19], the downshift of position of $\nu(C-S)_G$ and $\nu(C-S)_T$ modes is noticed

Table 2. Experimental and calculated Metal−S and C−S wavenumbers for MHP adsorbed at Au and Ag electrodes and calculated corresponding bond lengths.

Bond	System	Vibrational mode	Experimental Wavenumber (cm^{-1})	Calculated Wavenumber (cm^{-1})	Calculated bond length (pm)
C−S	MHP[a]	$\nu(C-S)_G$	655	n.a.	n.a.
	MHP[b]	$\nu(C-S)_T$	732	736	184.37
	Au/MHP	$\nu(C-S)_T$	696	695	183.64
	Ag/MHP	$\nu(C-S)_T$	692	704	182.81
	Ag/MHP	$\nu(C-S)_G$	630	n.a.	n.a.
Au−S	Au/MHP	$\nu(Au-S)$	260	255	235.45
Ag−S	Ag/MHP	$\nu(Ag-S)$	236	230	257.73

[a] Measured in 0.5 M MHP aqueous solution; [b] measured in solid state.
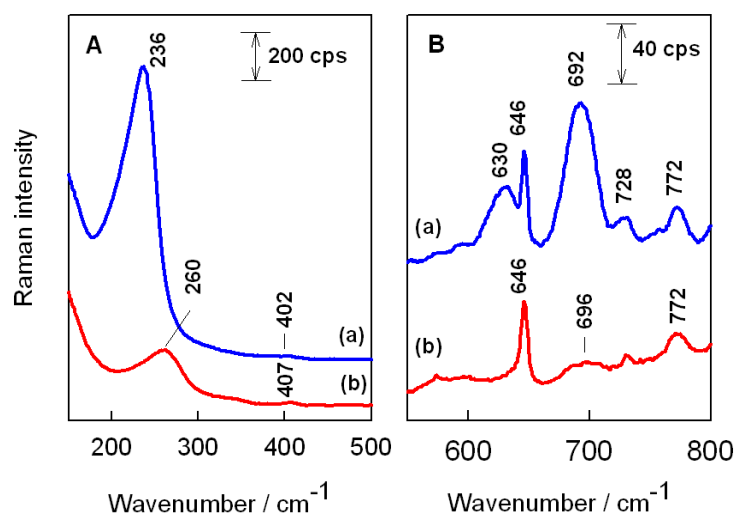
Fig. 4. SERS spectra of (a) Ag/MHP and (b) Au/MHP monolayers in metal−sulfur (A) and C−S (B) stretching frequency regions. Intensities were normalized according to the intensity of pyridinium ring ν_{6b} mode at 646 cm^{-1}. For clarification spectra were sifted vertically.

Dependence on adsorption time

For understanding of molecular ordering, orientation, and interaction strength between the neighboring molecules were performed adsorption time dependence

measurements. SERS spectra were recorded at different immersion times in adsorption solution (Fig. 5). Several minor changes in parameters of the SERS bands were observed, and difference spectra revealed the most sensitive bands to the changes in monolayer structure upon increasing time of self-assembly. We observed increasing frequencies of these peaks: ν(C–N) + β(CH) mode near 1171–1174 cm^{-1}, ν_{8a} near 1625–1628 cm^{-1}, also increased peak frequency of ν(Au–S) mode at 266–258 cm^{-1} and appeared the positive peak near 276 cm^{-1} which indicates that the higher frequency component decrease with increasing adsorption time. Besides we observed increasing in 1084 cm^{-1} band, and disappearance of the band at 2832 cm^{-1}. The latter band is assigned to soft C–H stretching mode of methylene groups and indicates direct interaction of CH$_2$ groups with the electrode surface at short immersion times.
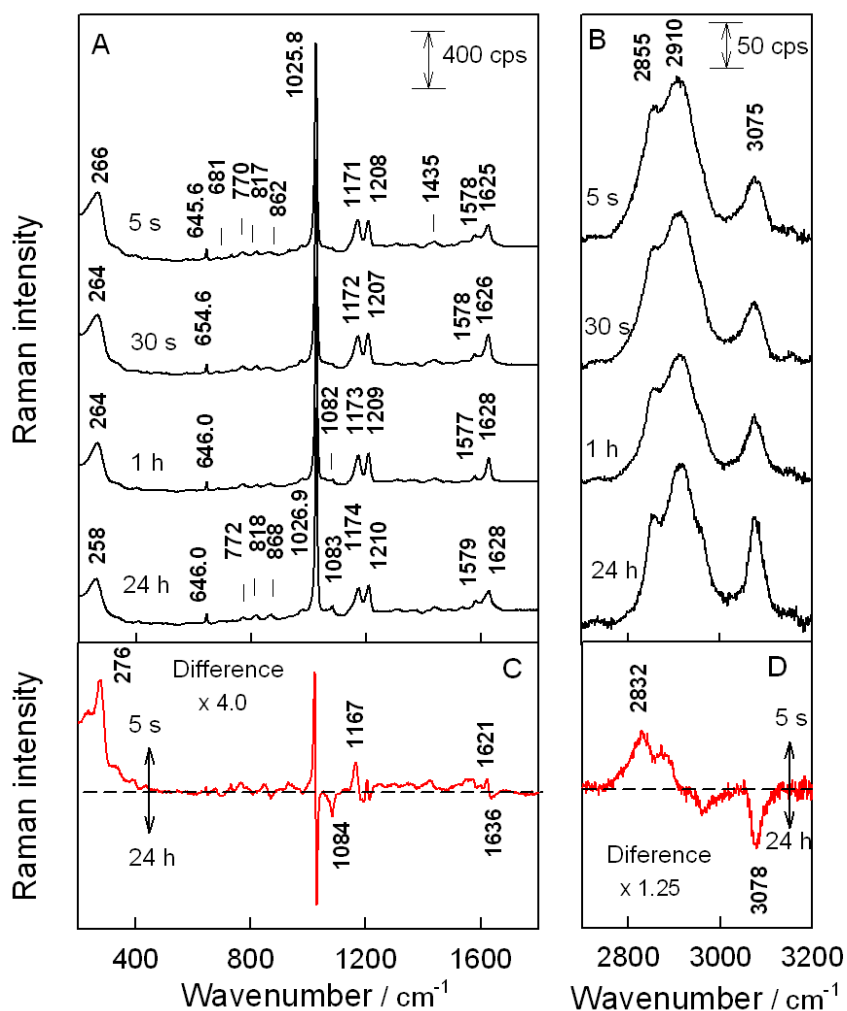
Fig. 5. SERS spectra of MHP adsorbed at gold electrode in (A) 100–1700 cm^{-1} and (B) 2750–3200 cm^{-1} spectral regions obtained at different immersion times in acetonitrile solution containing 10^{-3} M MHP, and corresponding difference spectra (C, D). Spectra are recorded at Au/MHP/air interface. Excitation wavelength is 785 nm.

Temperature dependence

To get deeper understanding on conformational changes of the hydrocarbon chain and intermolecular interactions between the chains of MHP, temperature dependent experiments were conducted (Fig. 6). During increase in temperature from 5 to 80 $^{\circ}$C we observed 1) considerable decrease in $\nu(=C-H)$ mode frequency (by 7 cm^{-1}), 2) increase in methylene $\nu_{as}(CH_2)$ frequency (by ~ 5 cm^{-1}), 3) slight decrease in the most intense ν_{12} mode frequency (by 0.7 cm^{-1}) and increase in this band intensity, 4) decrease in intensity of 1084 cm^{-1} band, 5) decrease in frequency of $\nu(C7-N1) + \beta(CH)$ mode near 1177 cm^{-1} (by 3 cm^{-1}), and 6) downshift of $\nu(Au-S)$ mode frequency. The increase in intensity and frequency of $\nu_{as}(CH_2)$ band might be associated with formation of intrachain gauche defects at higher temperatures. Difference spectrum clearly reveals broad positively-going feature near 2920 cm^{-1} associated with increase in intensity of $\nu_s(CH_2)_{FR}$ mode. The downshift in $\nu(Au-S)$ band frequency indicates weakening of the interaction strength between sulfur atom and gold surface.

To understand origin of feature near 1084 cm^{-1} we measured SERS spectra of MHP and ring deuterated analogue MHP-D$_5$ in the frequency region of 960–1700 cm^{-1} also carefully inspected wavenumber region between 1050 and 1100 cm^{-1} (Fig. 7). The ring bands at 1633, 1583, 1211, 1175, and 1028 cm^{-1} downshift to 1592, 1552, 868, 1133 and 989 cm^{-1}, respectively (Table 1), and the bands located at 1440 and 1083 cm^{-1} remain unshifted indicating that these modes belong to vibration of hydrocarbon chain. The 1440-cm^{-1} peak is associated with scissoring bending mode of methylene groups, $\delta(CH_2)$, while the peak at 1083 cm^{-1} falls in the frequency region typical for hydrocarbon chain C–C stretching vibrations. Figure 7B clearly shows that intensity of 1084 cm^{-1} peak increases with lowering the temperature. Calculations also predicted an intense Raman band at 1083 cm^{-1} for in-phase C–C stretching vibration of hydrocarbon chain in all-trans conformation (Table 1). Based on these arguments the 1084 cm^{-1} peak was assigned to $\nu(C-C)_T$ vibrational mode of hydrocarbon chain in all-*trans* conformation.
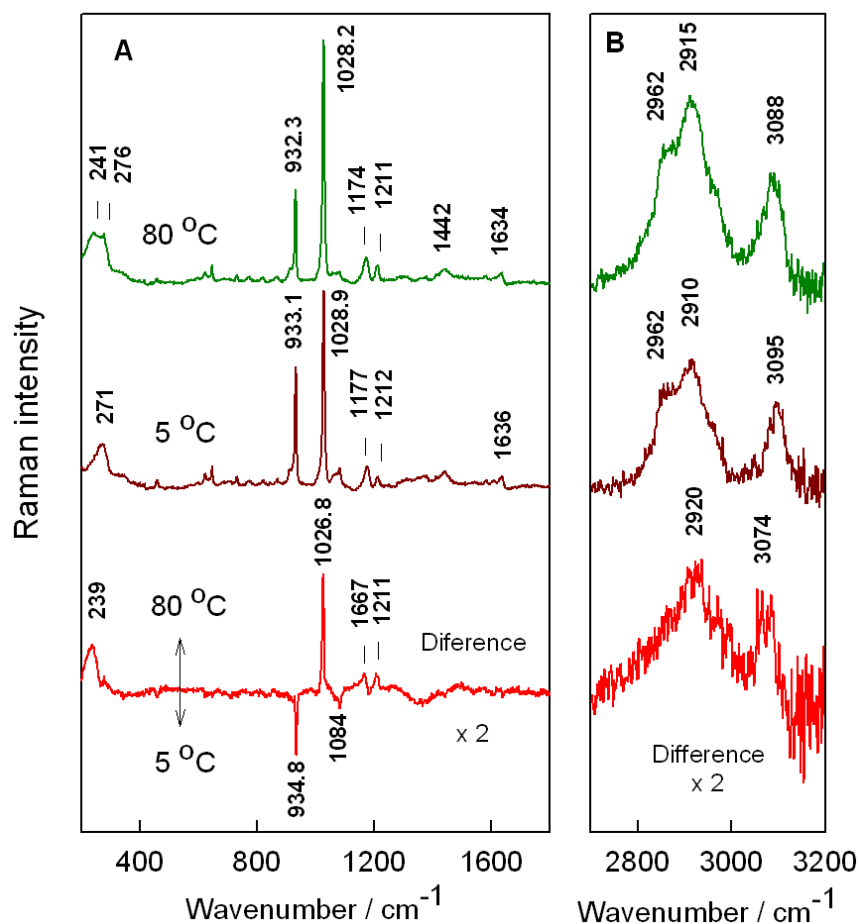
Fig. 6. SERS spectra of MHP monolayer on Au electrode in 0.1 M NaClO$_4$ solution at 80 and 5 ^{o}C temperature in 200–1700 cm^{-1}(A) and 2700–3200 cm^{-1} (B) spectral regions. The difference spectra are also shown.
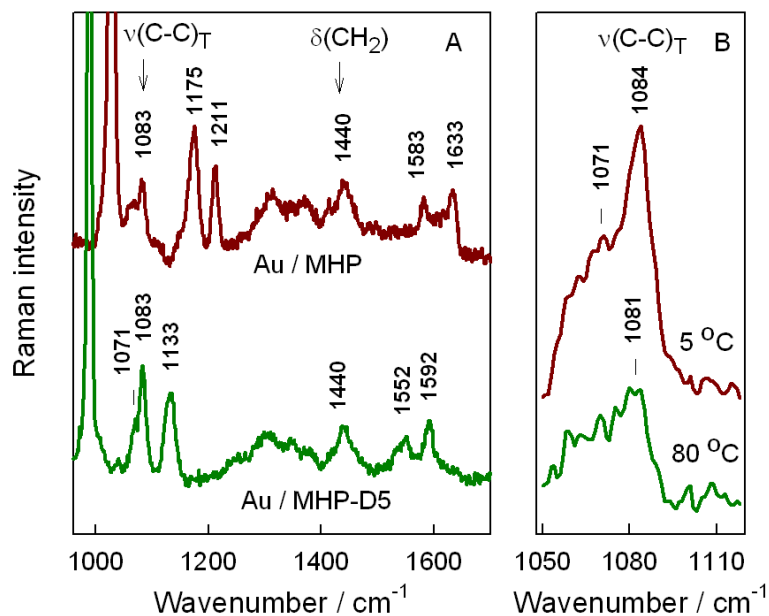
Figure 7. SERS spectra MHP and MHP-D$_5$ adsorbed at Au electrode in frequency region of 960–1700 cm^{-1} (A), and temperature dependence of SERS spectra of MHP in the frequency region of 1048–1120 cm^{-1} (B).

19

SERS marker bands of MHP structure and orientation on metal surface

Table 3 summarizes the experimental results concerning the SERS marker bands of MHP structure and orientation with respect to the electrode surface.

Table 3. SERS conformational marker bands of MHP structure and orientation

| Marker	Mode frequency and assignment	Molecular group	Sensitivity of the marker
$I[\nu_2]/I[\nu_{as}(CH_2)]$	2910 cm^{-1}, CH$_2$ asymmetric stretching/ 3080 cm^{-1}, =(C−H) stretching	Pyr/hydrocarbon chain	Orientation of molecule with respect to the surface, intensity ration increases for more perpendicular alignment
$\nu_{as}(CH_2)$	2910 cm^{-1}, CH$_2$ asymmetric stretching	Hydrocarbon chain	Intrachain order, frequency decreases with increasing ordering
$I[\nu(C−H)soft]$	2830 cm^{-1}, C−H stretching	Hydrocarbon chain	Interaction of CH$_2$ groups with surface; Intensity increases with increasing number of CH$_2$ groups interacting with surface
ν_{8a}	1635 cm^{-1}, ν(C2=C3)+ν(C6=C5)	Pyr	Interaction between the rings, frequency increases with increasing interaction strength
ν(C7−N1) + β(CH)	1174 cm^{-1}	Pyr−alkyl chain bond	Interaction between the rings, frequency increases with increasing interaction strength
$I[\nu(C−C)_T]$	1083 cm^{-1}, C−C in-phase stretching vibration (all-*trans*)	Hydrocarbon chain	Intrachain order, intensity increases with increasing number of all-trans conformers
$I_{\nu(C−S)T}/I_{\nu(C−S)G}$[a]	692 cm^{-1}/630 cm^{-1}, C−S stretching	thiolate	*Trans/gauch* isomerization
ν(Au−S)/ν(Ag−S)	260 cm^{-1}/230 cm^{-1}	metal−sulfur bond	Interaction strength with metal

[a]Peak positions determined for MHP adsorbed at Ag electrode.

The peak at 1083 cm^{-1} was recognized as a marker band for all-*trans* configuration of C−C bonds. It should be noted that calculations show that this mode corresponds to in-phase vibration of all C−C bonds in *trans* configuration. The appearance of soft C−H mode near 2830 cm^{-1} in SERS spectra shows direct interaction of methylene groups from hydrocarbon chain with the metal surface. The frequency of $\nu_{as}(CH_2)$ band at 2910 cm^{-1} increases with increasing temperature (Fig. 5) indicating decrease in the interaction between the chains and intrachain order. Possibility to monitor the interaction strength of MHP with the electrode provides low frequency metal−sulfur stretching vibration.

Higher frequency in the case of ν(Au−S) mode comparing with ν(Ag−S) correlates with shorter (stronger) Au−S bonding.

Increasing immersion time and temperature results in upshift of both ν(C−N)+β(CH) and ν_{8b} frequencies, indicating possibility to use these modes as markers for analysis of interaction between the pyridinium rings. The depolarized ring deformation mode ν_{6b} might be employed as intensity or frequency standard in analysis of MHP SERS spectra, because it was least sensitive to variations in temperature or immersion time.

Spectroelectrochemistry of MHP

Potential dependent studied have shown drastic changes in relative intensities of the SERS bands (Fig. 8 (A)); relative intensity of ring ν_{8a} mode near 1634 cm^{-1} was found to increase comparing with totally symmetric ring mode ν_{1a} at 1029 cm^{-1}. Experiments performed with different excitation wavelengths revealed increase in relative intensity of ν_{8a} mode at shorter wavelengths (Fig. 9). Such behavior is typical for systems where the operation of an addition SERS enhancement mechanism, called Charge transfer excitation, takes place. In addition, potential-difference spectra have indicated the appearance of soft C–H stretching mode near 2835 cm^{-1} at more negative potentials (Fig. 10). Presence of this mode indicates on the direct interaction of methylene groups of hydrocarbon chain of MHP as the electrode potential becomes more negative. One may expect that in this configuration the pyridinium ring lies closer to the electrode surface, thus facilitating the charge transfer excitation process. Such scenario was indeed confirmed experimentally by potential-dependent studies of mixed MHP:HPT (1:2, concentration ratio in adsorption solution of MHP and heptanethiol) monolayer (Fig. 11). One can see that relative intensity I_{1630}/I_{1029} at certain sufficiently negative electrode potential decreases for mixed monolayer indicating suppression of SERS enhancement due too the Charge transfer excitation mechanism.
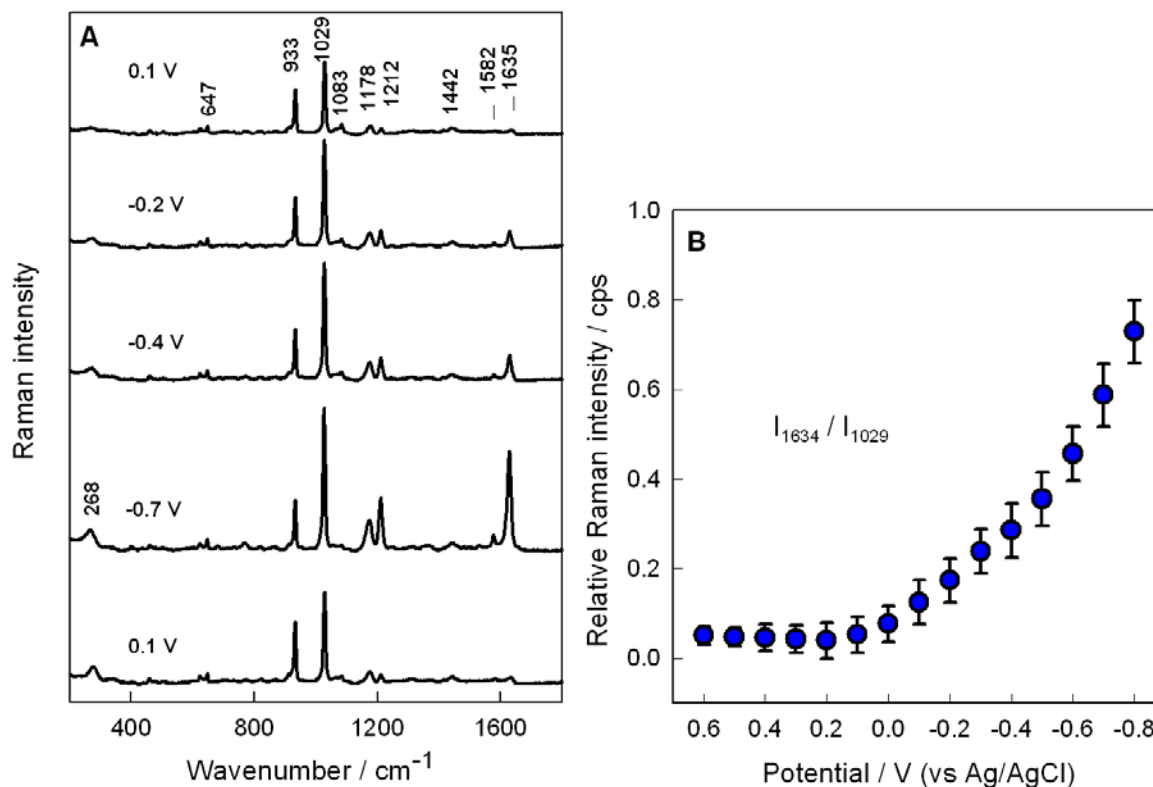
Fig. 8. Dependence of SERS spectra of MHP on potential (A) and dependence of relative intensity of ν_{8a} band near 1634 cm^{-1} and ν_{1a} band at 1029 cm^{-1} on potential (B). Spectra are recorded in 0.1 NaClO$_4$ M solution. Excitation wavelength is 785 nm.
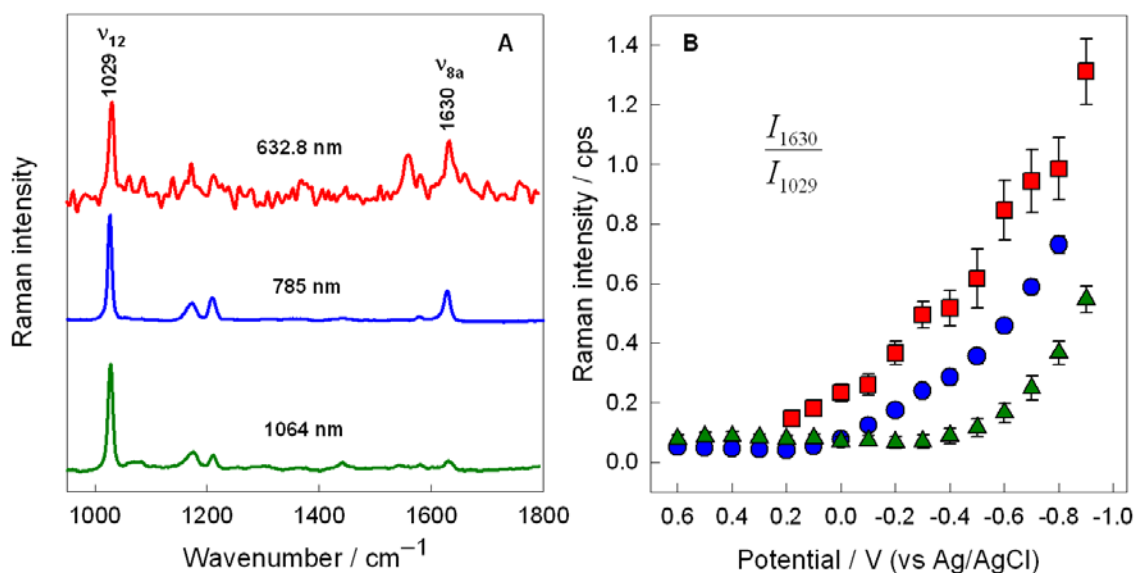
Fig. 9. Dependence of SERS spectra of MHP on excitation wavelength (A) and dependence of relative intensity I_{1630}/I_{1029} on the electrode potential at different excitation wavelengths. Spectra are recorded in 0.01 NaClO$_4$ M solution.

22
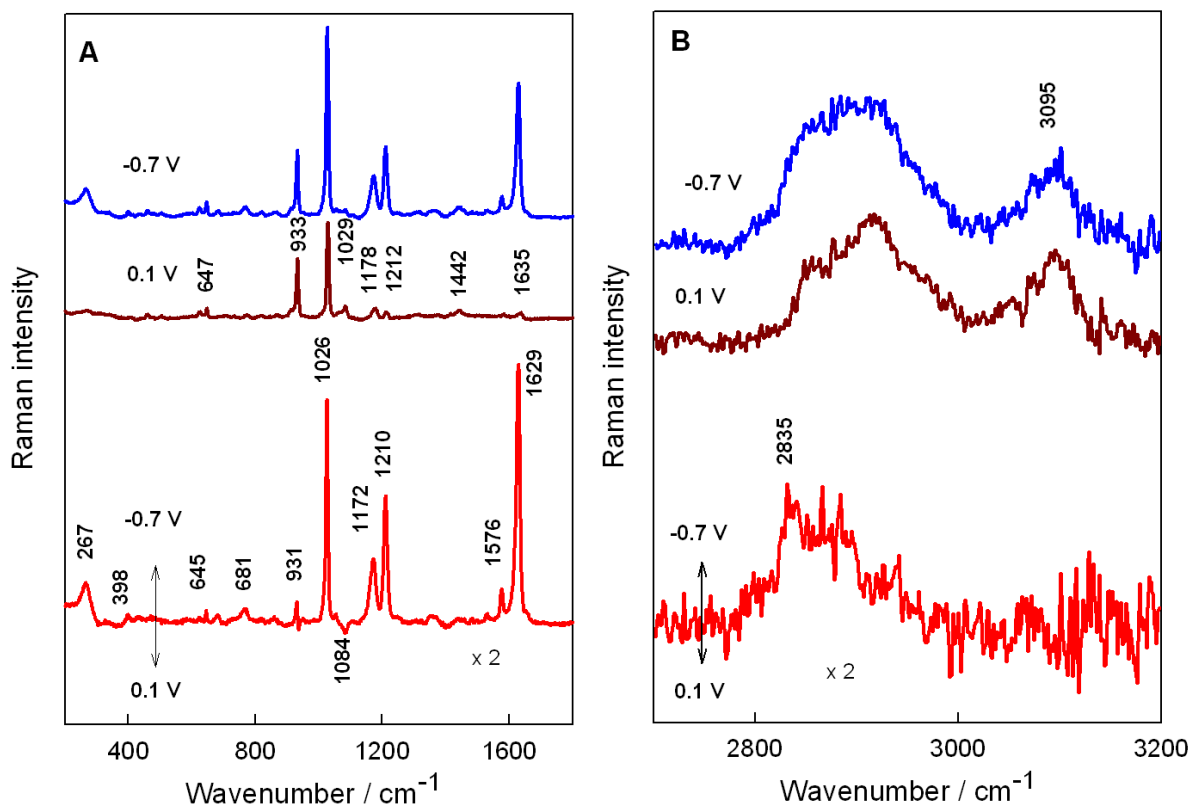
Fig. 10. Dependence of SERS spectra of MHP on potential in fingerprint (A) and high frequency (B) spectral regions. Soft C–H stretching mode is visible near 2835 cm^{-1} in the spectrum recorded at –0.70 V.
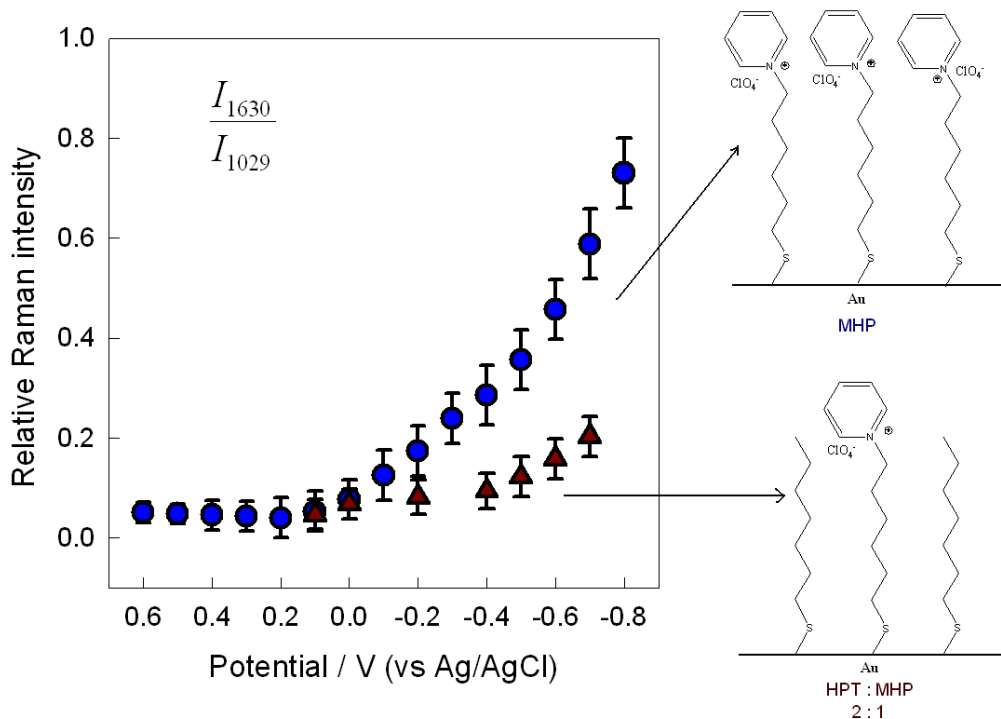
Fig. 11. Dependence of MHP and MHP: HPT mixtures of relative intensity of ν_{8a} near 1634 cm^{-1} and ν_{1a} at 1029 cm^{-1} on potential

MHP interaction with inorganic anions

The ability of MHP monolayer to attract ions from the solution phase (function of the monolayer) is demonstrated in Figure 12, which compares SERS spectra of MHP adsorbed on Ag electrode acquired in aqueous solution containing 0.01 M of SO_4^{2-} and ClO_4^- anions. As can see in difference spectrum intense positive-going peak at 933 cm^{-1} and low intensity negative-going band at 978 cm^{-1} are associated with totally symmetric vibrations of ClO_4^- and SO_4^{2-} anions, respectively [27, 28]. Analysis on these peaks shows that totally symmetric stretching vibrations for ClO_4^- and SO_4^{2-} anions in solution Raman spectrum is similar, $I_R(ClO_4^-)/I_R(SO_4^{2-}) = 0.90$, while for surface bound anions the relative intensity in SERS spectrum was found to be $I_{SERS}(ClO_4^-)/I_{SERS}(SO_4^{2-}) = 36$. This means that ClO_4^- anions preferentially bind to MHP monolayer comparing with SO_4^{2-} ions.

Fig. 13 shows the dependence of difference SERS spectra on the nature of solution anion. Positive-going peaks correspond to totally symmetric stretching vibrations of $NH_2SO_3^-$, SO_4^{2-}, NO_3^-, BF_4^-, ClO_4^-, and PF_6 anions electrostatically attracted by MHP monolayer on Au and Ag surfaces. Analysis of relative intensities of surface attracted anions reveals that anions with lower Gibbs dehydration energy are preferentially attracted by the MHP monolayer, and the peak positions of surface bound anions are slightly lower as comparing with the solution phase data (Table 4). Importantly, the downshift is higher for anions exhibiting larger Gibbs dehydration energy. Such frequency shift might be associated with deformation of solvation shell of the anions upon interaction with pyridinium ring. The more pronounced deformation is expected for higher solvated anions.
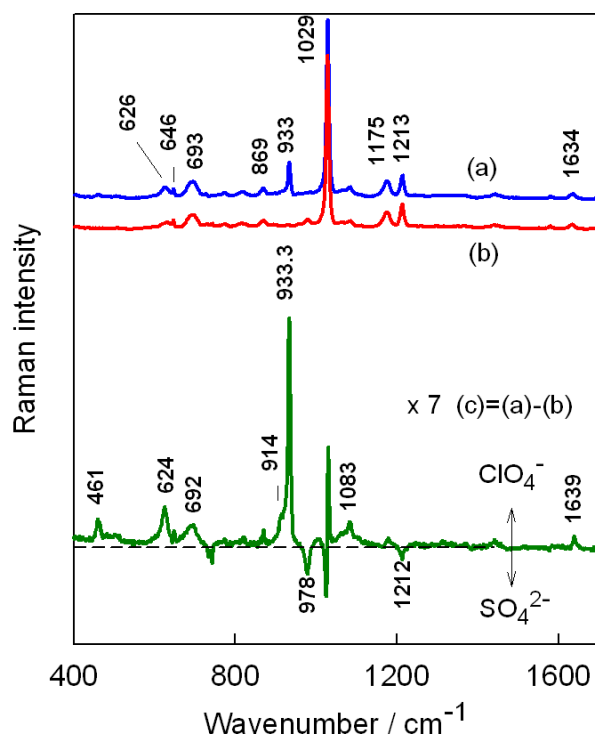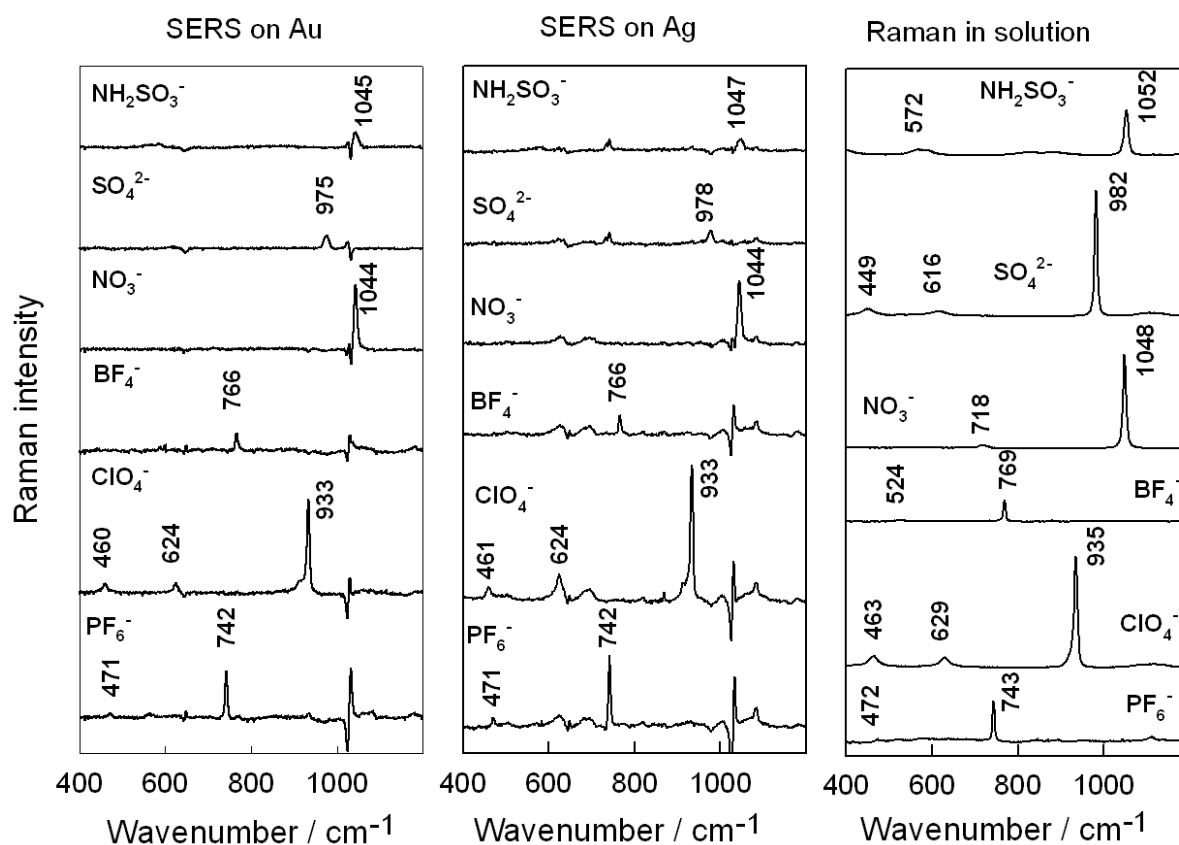
Fig. 12. SERS spectra of MHP monolayer on Ag electrode in (a) 0.01 M Na_2SO_4 and (b) 0.01 M $NaClO_4$ aqueous solutions. Difference spectrum (c) is also shown. The excitation wavelength is 785 nm.

Table 4. Gibs hydration energies (kJ mol^{-1}) and peak positions (cm^{-1}) of symmetric stretching vibration of anions in solution Raman and SERS spectra, and corresponding frequency-difference Δ (cm^{-1}) values

| Anion	Gibbs dehydration energy[a]	Peak position		$\Delta = \nu_{Raman} - \nu_{SERS}$
		Raman	**SERS**	
$NH_2SO_3^-$	–	1052.6	1046.9	5.7
SO_4^{2-}	1080	982.0	977.6	4.4
NO_3^-	300	1048.3	1044.2	4.1
BF_4^-	–	769.0	765.5	3.5
ClO_4^-	205	934.9	933.3	1.6
PF_6^-	–	743.3	741.8	1.5

[a]From reference [29].

Fig. 13. Dependence of the difference SERS spectra of MHP monolayer on Au and Ag electrodes on the nature of the solution anion. The difference spectra were constructed by subtraction the spectrum obtained in 0.01 M NaF solution from that recorded in 0.01 M Na_mX, where X^{m-} = $NH_2SO_3^-$, SO_4^{2-}, NO_3^-, BF_4^-, ClO_4^-, or PF_6^-. The difference spectra were normalized to the intensity of ν_{12} mode near 1030 cm^{-1}. Excitation wavelength is 785 nm.

Other measurements were performed to define the detection limit of ClO_4^- ions in solution by using SERS method and MHP monolayer. Fig. 14A demonstrates that adsorbed ClO_4^- became visible in SERS spectrum at 10^{-8} M concentration in solution. The dependence of SERS intensity on concentration is linear in the concentration range from 10^{-8} to 10^{-3} M (Fig. 14B). In addition, we found that the frequency of this band depends on the adsorption time of anion from the diluted solution (Fig. 15). This indicates that solvation shell of the anion is more perturbed at the initial adsorption stage.
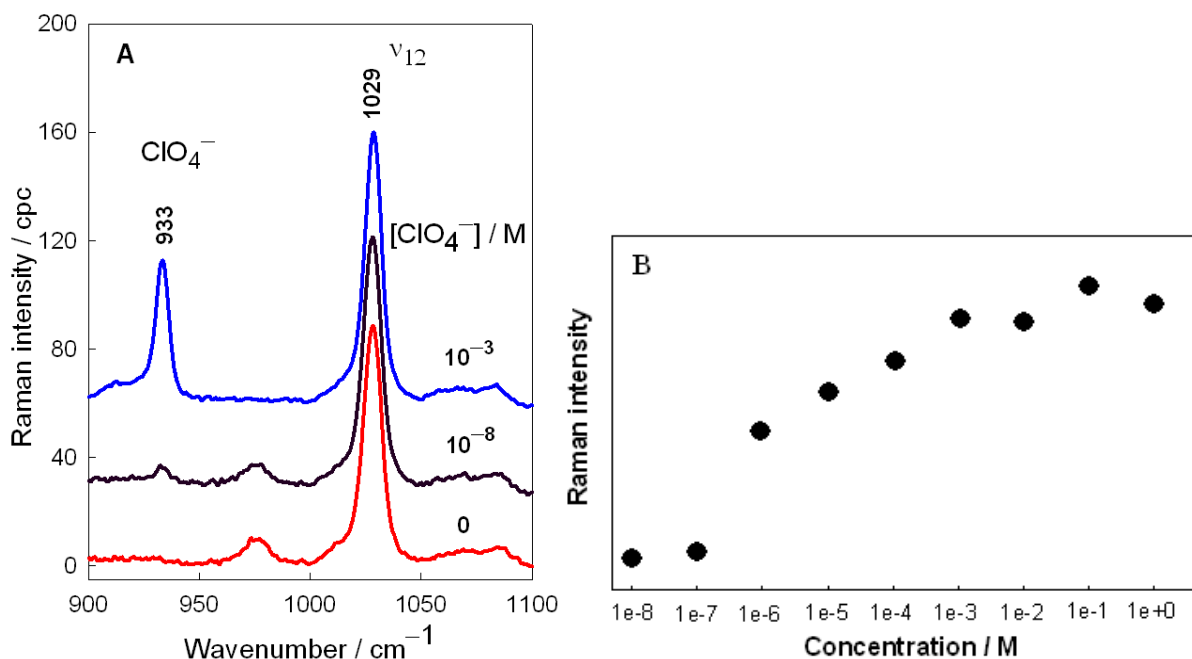
Fig. 14. *SERS spectra* of MHP monolayer at Au electrode at 0, 10^{-8}, and 10^{-3} M ClO_4^- concentrations (A). Dependence of intensity of totally symmetric stretching vibration of adsorbed ClO_4^- on the anion concentration in solution (B). The excitation wavelength is 785 nm.
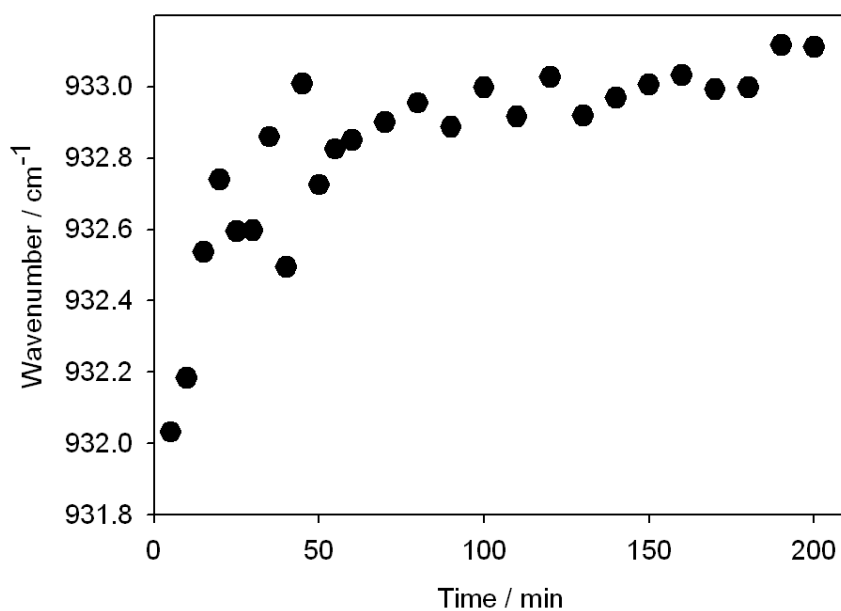

Fig. 15. Dependence of the wavenumber of the symmetric stretching vibration of ClO_4^- ions on the adsorption time at the MHP monolayer on gold electrode from aqueous 10^{-6} M $NaClO_4$ solution. Excitation wavelength is 785 nm.

MHP interaction with sodium dodecylsulphate

MHP forms ionic pairs not only with inorganic anions but also with organic dodecylsulphate (DS^-). While SERS feature at 933 cm^{-1} is clearly visible after introduction of ClO_4^- ions at 10^{-6} M concentration in solution (Fig. 16A, a), only minor

changes are visible in the SERS spectrum after introduction of SDS at the same concentration (Fig. 16B, a) However, difference spectrum revealed characteristic vibrational modes of DS⁻ (Fig. 16c). Thus, DS⁻ ions might be detected by SERS technique and MHP monolayer at 10^{-6} M concentration in solution. More detailed analysis of SERS spectra were performed at 10^{-3} M solution concentration of DS⁻ (Fig. 17). We carefully inspected the wavenumber region between 1040 and 1700 cm^{-1}. The most interesting bands were located at 1061 and 1366 cm^{-1}, and have been assigned to $\nu_s(SO_3) + \nu(C6–O4) + \nu(C–C)$ and $w(CH_2)$ (wagging mode) near SO_4 group, respectively. Comparing difference SERS spectrum with SDS solid state Raman spectrum one can see that adsorption induces an increase in relative intensity of I_{1366}/I_{1441} and downshift in $\nu_s(SO_3)$ band frequency (from 1063 to 1061 cm^{-1}). These spectroscopic changes indicate that the adsorbed DS⁻ ions interact with the MHP monolayer through the SO_3 group.
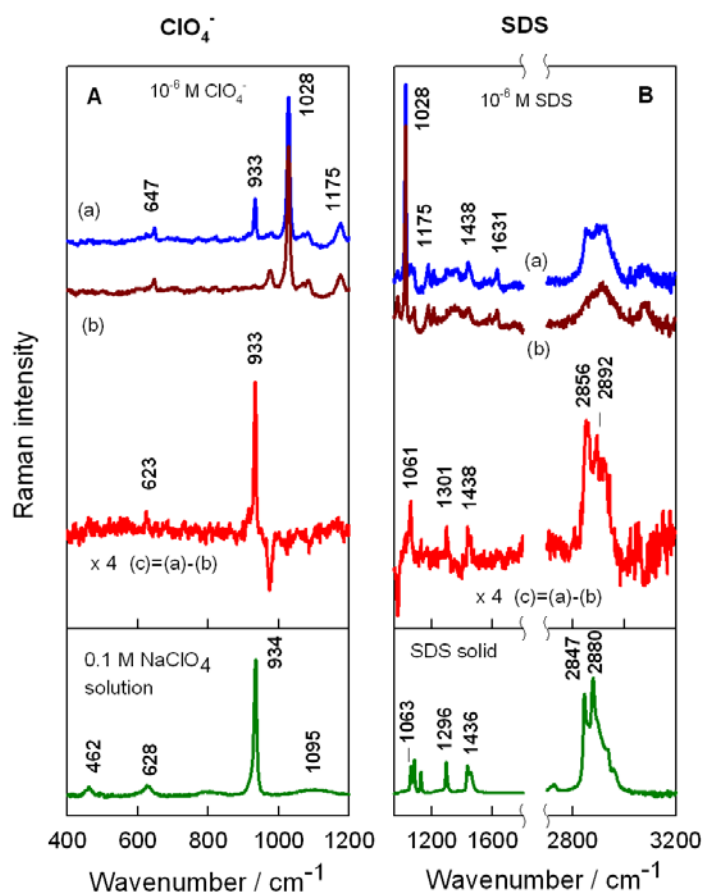
Fig. 16. SERS observation of formation of ion pairs between the pyridinium group of MHP monolayer on Au electrode and ClO_4^- (A) or DS⁻ (B) ions from the solution phase. SERS spectra after introduction (a) and before the introduction (b) of ions into the solution. Difference spectra (c) are also shown. Difference spectra were normalized to the intensity of ν_{12} mode near 1028 cm^{-1}. Excitation wavelength is 785 nm.
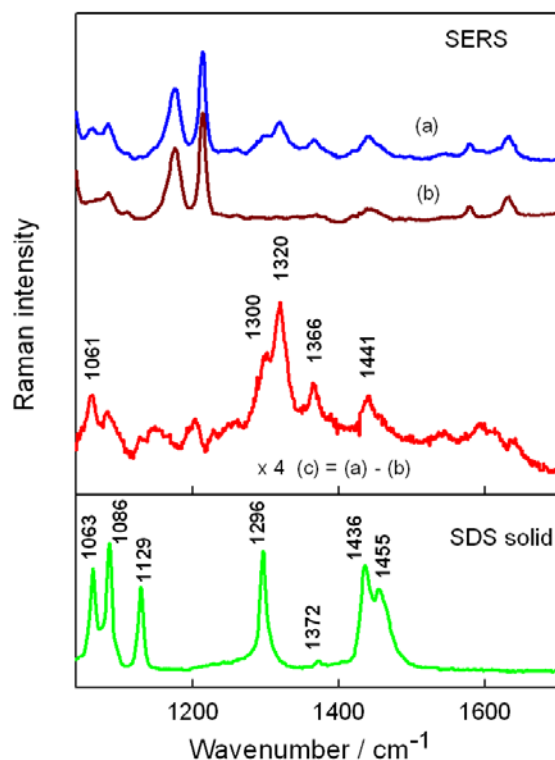
Fig. 17. SERS spectra of MHP monolayer on Ag electrode with (a) and without (b) of DS$^-$ at 10^{-3} M concentration in solution. The difference spectrum (c) is also shown. Raman spectrum of SDS in solid state is shown at the bottom. The difference spectra were normalized to the intensity of ν_{12} mode near 1030 cm^{-1}. Excitation wavelength is 785 nm.

### MHP interaction with grapheme oxide (GO)

MHP monolayer electrostatically attracts GO; interaction goes through the MHP pyridinium ring and carboxyl groups of GO (Fig. 18). Adsorption of GO at the Au/MHP is evidenced by the appearance of broad and characteristic features near 1322 and 1599 cm^{-1} associated with D and G modes, respectively (Fig. 18a). Clearly visible MHP bands, indicate that the adsorption of GO does not remove the initial monolayer from the surface. Furthermore, the intensity of MHP bands increased; it can be comparable to the recently observed enhancement of Raman bands by GO [30]. This observation indicates that MHP molecules directly interact with GO, as direct contact requared for the enhancement.

Second series of experiments were performed in solution containing 0.01 M NaF. We converted adsorbed GO to reduced graphene oxide (rGO) by cathodic polarization at −0.90 V for 600 s, and probed the dependence of parameters of vibrational bands (Fig. 19a). Different spectra clearly show shifts in the position of both D and G peaks to lower wavenumbers as the potential becomes more negative. For more quantitative analysis of

29

SERS bands spectra were fitted with *Gausian-Lorentzian* form components (Fig.19b). The broad and low intensity feature near 1556 cm^{-1} might be assigned to disorder–induced first order Raman scattering [31].
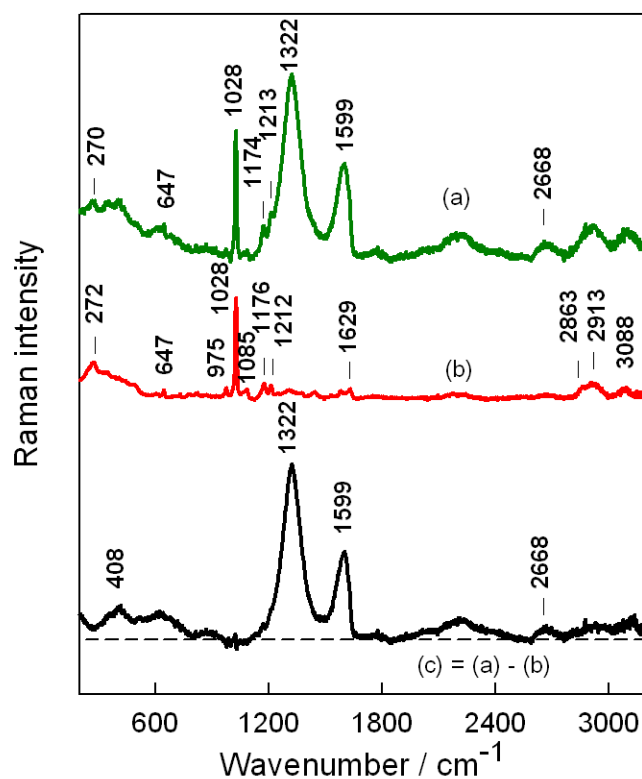

Fig. 18. SERS spectra from Au/MHP monolayer in aqueous solution (a) after, and (b) before the introduction of GO into the spectroelectrochemical cell. Difference spectrum (c) is also shown. In subtraction procedure spectra were normalized according to the intensity of ν_{12} peak of pyridinium ring at 1028 cm^{-1}.
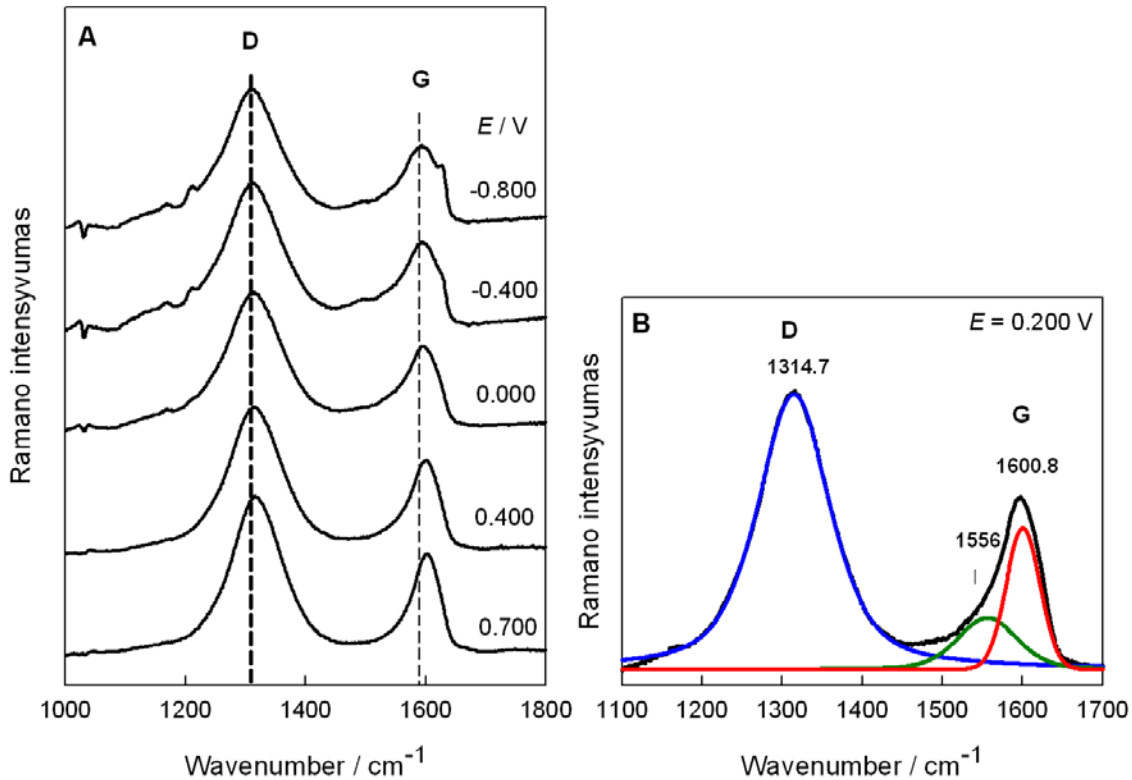
Fig. 19. Difference SERS spectra of rGO adsorbed at Au/MHP surface in solution containing 0.01 M NaF at indicated potentials (A). Fitting of difference Au/MHP/rGO SERS spectrum with Gausian-Lorentzian form components (B). During subtraction spectra were normalized according to the intensity of ν_{12} peak of pyridinium ring at 1028 cm^{-1}. Spectra were obtained after cathodic polarization at −0.90 V.

The variations of peak parameters for D and G modes on the potential are plotted in Fig. 20. The linear increase in peak frequencies as potential becomes more positive was observed, apparent frequency tuning rate was found to be 4.7 ± 0.3 cm^{-1}/V and 5.9 ± 0.3 cm^{-1}/V for D, and G modes, respectively (Fig. 20A,B). Intensity ratio I_D/I_G and full width at half maximum (FWHM) are affected by the potential as well. We found that bands of rGO become narrower at more positive electrode potentials (Fig. 20C). The dependence on FWHM of D and G bands is near linear in the potential region from −0.40 to 0.70 V, and generally it decrease of ~ 8 and 18 %, respectively, upon switching the potential from −0.90 to 0.70 V. Similarly, the I_D/I_G ratio was found to decrease from 2.1 to 1.8 as electrode potential was changed from −0.90 to 0.70 V. Considering the mechanism of potential induced perturbations in parameters of reduced GO bands, we have demonstrated that the dominant effect causing the frequency shift of D and G bands with the electrode potential is the change in the C−C bond strength induced by the electrochemical doping. Constructed in this work Au/MHP/rGO system is stable in

31

neutral aqueous solutions and it was demonstrated that the electrochemical potential controls the electronic properties of rGO. This system might be utilized in various electrochemical applications.
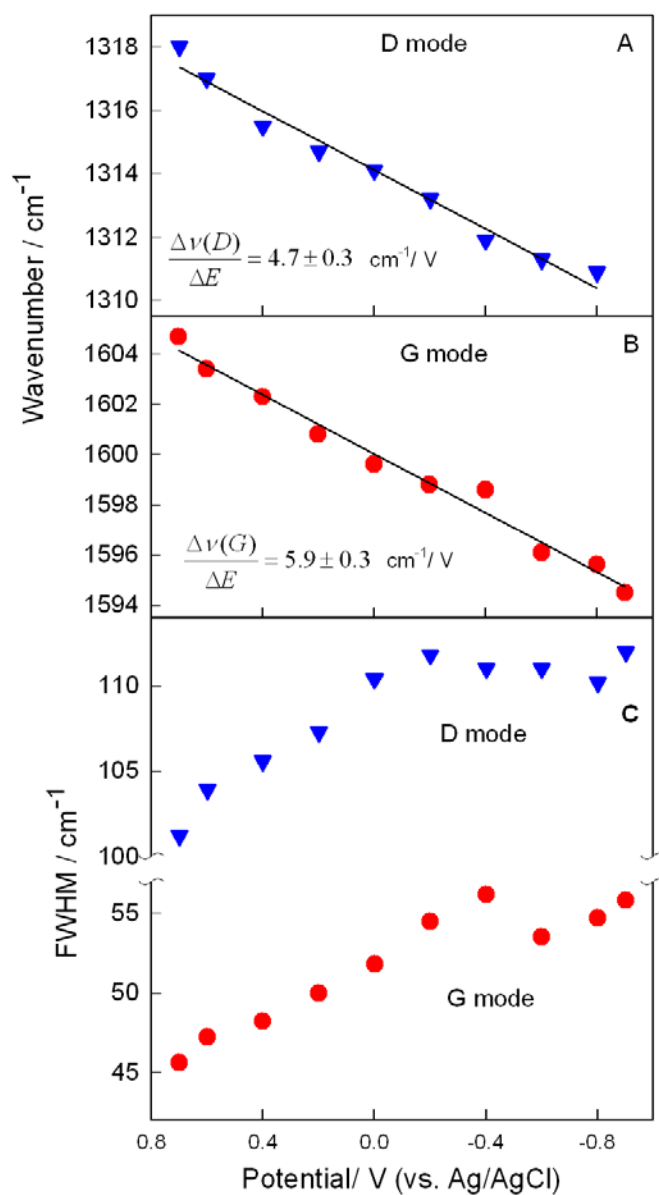
Fig. 20. Potential dependence of D-peak (A), and G-peak (B),and FWHM of D and G modes positions, of rGO adsorbed on Au modified by MHP monolayer in solution containing 0.01 M NaF. The lines are least-square fit by linear function.

CONCLUSIONS

1. N-(6-mercapto)hexylpyridinium (MHP) molecules form stable positive-charge-bearing self-assembled monolayers capable of attracting negatively charged molecules from the solution phase.

2. Raman markers for structure and orientation of MHP molecule have been established based on isotopic substitution, quantum chemical calculations, and adsorption time- and temperature-dependent studies. A band near 1083 cm^{-1} has been assigned to C–C stretching vibration of hydrocarbon chain in all-*trans* conformation.

3. As the electrode potential becomes more negative, changes in the orientation of MHP with respect to the surface takes place so that the methylene groups of hydrocarbon chain contact the metal and the relative intensity of the pyridinium ring mode ν_{8a} increases. The dependence of relative intensity $I(\nu_{8a})/I(\nu_{12})$ on the electrode potential and excitation wavelength was observed indicating on the operation of an additional charge transfer resonant Raman enhancement mechanism in Au/MHP system.

4. MHP monolayer electrostatically attracts $NH_2SO_3^-$, SO_4^{2-}, NO_3^-, BF_4^-, ClO_4^-, and PF_6^- anions. The frequency of totally symmetric stretching vibration of adsorbed ions decreases comparing with the corresponding mode of ions in solution. The higher shift corresponds to the larger Gibbs dehydration energy of the anion.

5. MHP monolayer on gold electrode provides possibility to determine the concentration of ClO_4^- ions in solution at a level of 10^{-8} M by probing the totally symmetric stretching vibration at 933 cm^{-1}. The dependence of SERS intensity on concentration is near linear in the concentration range from 10^{-8} to 10^{-3} M. The downshift in frequency of totally symmetric stretching mode for adsorbed ion depends on the solution concentration and decreases with increasing the concentration.

6. Interaction of MHP monolayer with dodecyl sulfate (DS$^-$) anions results in formation of bilayer at the interface. DS$^-$ anions can be detected by PSRS method at 10^{-6} M solution concentration. The decrease in frequency and increase in relative intensity of symmetric stretching vibration of sulfate group for adsorbed DS$^-$ indicates that interaction of MHP and the anion takes place through the sulfate group.

7. MHP monolayer electrostatically attracts negatively charged graphene oxide. Adsorbed graphene oxide can be reduced electrochemically. The frequencies of both G and D bands of reduced graphene oxide linearly decrease as electrode potential becomes more negative with slopes of 5.9 ± 0.3 and 4.7 ± 0.3 cm^{-1}/V, respectively. The effect was explained in terms of electrochemical doping induced changes in the C−C bonds length.

ACKNOWLEDGEMENTS

REFERENCES

1. A. Kudelski, W. Hill. *Langmuir.* 1999. **15**. 3162-3168.

2. B. Prieto-Simon, M. Campas, J-L. Marty. *Protein and Peptide Lett.* 2008. **15**. 757-763.

3. H-Y. Gu, A-M. Yu, H-Y. Chen. *J. Electroanal. Chem.* 2001. **516**. 119-126.

4. A. Kudelski. *Langmuir.* 2003. **19**. 3805-3813.

5. A. Michota, A. Kudelski, J. Bukowska. *Surface Science.* 2002. **502-503**. 214-218.

6. D. Zhou, X. Wang, L. Birch, T. Rayment, C. Abell. *Langmuir*, 2003. **19**. 10557-10562.

7. D. Zhou, A. Bruckbauer, M. Bachelor, D.-J. Kang, C. Abell, D. Klenerman. *Langmuir.* 2004. **20**. 9089-9094.

8. D. Zhou, A. Bruckbauer, C. Abell, D. Klenerman, D.-J. Kang. *Adv.Mater.* 2005. **17**. 1243-1248.

9. L. Porte-Peden, S. G. Kaamper, M.Vandr Wal, R. Blankespoor, K. Sinniah. *Langmuir.* 2008. **20**. 11556-11561.

10. W. S. Hummers, R. E. Offeman. J. *Am. Chem. Soc.* 1958. **80.** 1339–1339.

11. V. Vaičikauskas, G.-J. Babonas, Z. Kuprionis, G. Niaura, V. Šablinskas.: *TEV*, 2008. p. 186.

12. M.J. Frisch, G.W. Trucks, H.B. Schlegel, G.E. Scuseria, M.A. Robb, J.R. Cheeseman, J.A. Montgomery Jr., T. Vreven, K.N. Kudin, J.C. Burant, J.M. Millam, S.S. Iyengar, J. Tomasi, V. Barone, B. Mennucci, M. Cossi, G. Scalmani, N. Rega, G.A. Petersson, H. Nakatsuji, M. Hada, M. Ehara, K. Toyota, R. Fukada, J. Hasegawa, M. Ishida, T. Nakajima, Y. Honda, O. Kitao, H. Nakai, M. Klene, X. Li, J.E. Know, H.P. Hratchian, J.B. Cross, C. Adamo, J. Jaramillo, R. Gomperts, R.E. Stratmann, O. Yazyev, A.J. Austin, R. Cammi, C. Pomelli, J.W. Ochterski, P.Y. Ayala, K. Morokuma, G.A. Voth, P. Salvador, J.J. Dannenburg, V.G. Zakrzewski, S. Dapprich, A.D. Daniels, M.C. Strain, O. Farkas, D.K. Malick, A.D. Rabuck, K. Raghavachari, J.B. Foresman, J.V. Ortiz, A. Liashenko, P. Piskorz, I. Komaromi, R.L. Martin, D.J. Fox, T. Keith, M.A. Al-Laham, C.Y. Peng, A. Nanayakkara, M.

Challacombe, P.M.W. Gill, B. Johnson, W. Chen, M.W. Wong, C. Gonzalez, J.A. Pople, Gaussian 03, Revision D.01, Gaussian, Inc., Wallingford, CT, 2004.

13. L. Riauba, G. Niaura, O. Eicher-Lorka, E. Butkus.*J. Phys. Chem. A*. 2006. **110**. 13394–13404.

14. P.L. Polavarapu. *J. Phys. Chem*. 1990. **94.** 8106–8112.

15. G. A. Guirgis, P. Klaboe, S. Shen, D. L. Powell, A. Gruodis, V. Aleksa, C. J. Nielsen, J. Tao, C. Zheng, J. R. Durig. *J. Raman Spectrosc*. 2003. **34.** 322–336.

16. I. Matulaitienė, Z. Kuodis, O. Eicher-Lorka, G. Niaura. *J. Electroanal. Chem.* 2013. **700**. 77-85.

17. M. A. Bryant, J. E. Pemberton. *J. Am. Chem. Soc*. 1991. **113**. 8284–8293.

18. M. A. Bryant, J. E. Pemberton. *J. Am. Chem. Soc*. 1991. **113**. 3629–3637

19. A. Bulovas, N. Dirvianskytė, Z. Talaikytė, G. Niaura, S. Valentukonytė, E. Butkus, V. Razumas. *J. Electroanal. Chem.* 2006. **591**. 175–188.

20. K. M. Marzec, S. Jaworska, K. Malek, A. Kaczor, M. Baranska. *J. Raman Spectrosc.* 2013. **44.** 155–165.

21. P. A. Mosier-Boss, S. H. Lieberman. *Langmuir.* 2003. **19.** 6826–6836.

22. V. Voiciuk, G. Valincius, R. Budvytyte, A. Matijoska, I. Matulaitiene, G. Niaura. *Spectrochim. Acta A*. 2012. **95**. 526–532.

23. K. A. Bunding, M. I. Bell, R. A. Durst. *Chem. Phys. Lett*. 1982. **89.** 54–58.

24. E. Koglin, A. Tarazona, S. Kreisig, M.J. Schwuger. *Coll. Surf. A*. 1997. **123–124**, 523–542.

25. S.M. Kreisig, A. Tarazona, E. Koglin, M.J. Schwuger. *Langmuir*. 1996. **12**. 5279–5288.

26. I. Razmutė–Razmė, Z. Kuodis, O. Eicher–Lorka, G. Niaura. *Phys. Chem. Chem. Phys.* 2010. **12**. 4564–4568.

27. G. Niaura, A. Malinauskas. *J. Chem. Soc. Faraday Trans*. 1988. **94.** 2205–2211.

28. G. Valincius, G. Niaura, B. Kazakeviciene, Z. Talaikyte, M. Kazemekaite, E. Butkus, V. Razumas. *Langmuir.* (2004). **20**. 6631–6638.

124. A. Yuchi, S. Kuroda, M. Takagi, Y. Watanabe, S. Nakao. *Anal. Chem*., 2010. **82**, 8611–8617.

30. W. Liang, X. Chen, Y. Sa, Y. Feng, Y. Wang, W. Lin. *Appl. Phys. A*. 2012. **109**. 81–85.

31. L. Kavan, L. Dunsch.. *ChemPhysChem*. 2011. **12.** 47–55.

ADSORBUOTŲ ANT METALO PAVIRŠIAUS MONOSLUOKSNIŲ SU PIRIDINIO FUNKCINE GRUPE STRUKTŪROS IR SĄVEIKOS SU TIRPALO KOMPONENTAIS TYRIMAS VIRPESINĖS SPEKTROSKOPIJOS METODAIS

ANOTACIJA

Savitvarkiai monosluoksniai suteikia metalų paviršiams norimas savybes ir plačiai taikomi elektronų pernašos tyrimuose, konstruojant (bio)jutiklius, biotechnologinius bei fotoelektroninius procesus. Teigiamo krūvio monosluoksniai naudojami kuriant anijonų jutiklius ir (bio)technologinius procesus su adsorbuotomis neigiamo krūvio makromolekulėmis. Darbe buvo susintetinta bifunkcinė molekulė su galinėmis tiolio ir piridinio grupėmis, suformuotas monosluoksnis ir ištirtos jo struktūrinės ir funkcinės savybės.

Pagrindiniai darbo tikslai buvo ištirti N-(6-merkapto)heksilpiridinio (MHP) adsorbuoto ant Au ir Ag elektrodų struktūrą ir nustatyti monosluoksnio sąveikos su neorganiniais anijonais, dodecilsulfato anijonu ir grafeno oksidu dėsningumus.

Naudojant paviršiaus sustiprintos Ramano spektroskopijos, kvantų chemijos skaičiavimo ir izotopinio pakeitimo metodus nustatyti MHP struktūros ir orientacijos elektrodo atžvilgiu Ramano sklaidos žymenys. Tiriant juostų intensyvumo priklausomybes nuo potencialo ir žadinančios spinduliuotės bangos ilgio parodyta, kad Au/MHP sistemoje pasireiškia krūvio pernešimo Ramano spektrų stiprinimo mechanizmas. Nustatyta, kad adsorbuotų neorganinių anijonų pilnai simetrinio virpesio dažnis sumažėja lyginant su tirpalo spektru ir tas pokytis koreliuoja su Gibso dehidracijos energija. Parodyta, kad MHP pritraukia grafeno oksidą. Nustatyta, kad grafeno oksido C−C ryšio ilgis ir elektroninė struktūra gali būti keičiama, keičiant potencialą.

CURRICULUM VITAE

IEVA MATULAITIENĖ
1984–01–23, Vilnius

Contact address:

Center for Physical Sciences and Technology, Institute of Chemistry, A. Goštauto 9, LT-01108 Vilnius, Lithuania. Tel. 272 96 42

Email: ieva.kairyte@gmail.com

Education:

2008 – 2012	Doctoral studies at Institute of Chemistry, Center for Physical Sciences and Technology.
2006 – 2008	Vilnius Gediminas Technical University, master degree in bioengineering
2002 – 2006	Vilnius Gediminas Technical University, bachelor degree in bioengineering

Work/practice experience:

2013 – till now   Junior research associate, Center for Physical Sciences and Technology.

2013 – 2013 12 31   Specialist, Vilnius University.

2010 – 2013   Engineer, Center for Physical Sciences and Technology.

2009 – 2010   Engineer, Institute of Chemistry.

2008   Master degree final thesis: *Production and characterization of monoclonal antibodies against Hendra and Nipah virus nucleocapsid proteins*, supervisor: dr. A. Žvirblienė (Institute of Biotechnology).

2006 – 2008   Technician, Institute of Biotechnology.

2006   Bachelor degree final thesis: *Imaging virus-like particles by atomic force microscopy,* supervisor: prof. habil. dr. V. Snitka (KTU RC, Mycrosystems and Nanotechnology).

2005 July   Industrial internship, Customs Laboratory, Vilnius

2004 July   Training internship, Institute of Biotechnology, Vilnius.